Al-Mustansiriyah Journal of Science
ISSN: 1814-635X (print), ISSN:2521-3520 (online) Volume 33, Issue 4, 2022 DOI: http://doi.org/10.23851/mjs.v33i4.1203

Research Article Open Access

Pore Size Dependence of Optical Absorption Enhancement in Porous Anodic Aluminum Oxide

Riad M. Hameed, Ahmed Al-Haddad*, Abbas K. H. Albarazanchi

Department of Physics, College of Science, Mustansiriyah University, Baghdad, IRAQ.

*Correspondent contact: ahmed.al-haddad@uomustansiriyah.edu.iq

Article Info

Received
07/08/2022

Accepted
06/09/2022

Published
30/12/2022

ABSTRACT

Three samples of high ordered AAO template were prepared via a two-step anodization procedure, the pore size was modified during the pore-widening process to tune the pore diameter to 50, 70, and 90 nm. Scanning electron microscopy (SEM) was adopted to gauge the pore diameter and the cell unit of the periodical hexagonal structure of the prepared AAO templates. In addition, the UV-vis spectrometer shows the variation of the absorbance spectrum for each pore size of the prepared AAO templates. To prove that the pore diameter (P_D) and the intermediate layer (I_L) could enhance the absorbance of the materials, a Lumerical FDTD solution was used by involving the exact experimental conditions of the AAO template. The resulting data show that a specific pore diameter with a specific intermediate layer can improve the absorbance spectrum of the materials. Thus, the results could serve the applications related to solar energy conversion (antireflective and photocatalyst) and photonics.

KEYWORDS: AAO template; porous materials; FDTD; absorbance spectrum of Alumina; Lumerical solution.

INTRODUCTION

Pore array materials have their unique physical properties; therefore, a great interest is paid to investigating the characteristics of each controlled condition [1, 2]. Anodic aluminum oxide (AAO) templates are a perfect example of the simple utilization and high tunability of the arrays of the pore sizes, the structure of the AAO template is described in Figure 1a. Since the creation of highly organized nanostructure arrays is crucial. Although lithography has technical and financial constraints for large-scale integrated manufacturing in the upcoming stage of lower than 100 nm scale, self-organizing techniques have great attention to synthesis nanostructure [3-5]. Due to its unique properties, including controlling the periodical and diameter of the pores, high aspect ratio of pore size, and the preferable cylindrical form, AAO templates have drawn the most attention in synthetic nanostructure materials [6-11]. This provides a potentially effective way to create an ordered nanostructure with a large area and a high aspect ratio, which is very challenging to make via lithographic methods used today. However, when utilizing the conventional anodization process, the configuration of the pores is extremely haphazard. For specific sets of parameters, Masuda *et. al.* enhanced a two-step anodization technique, producing the ideal hexagonal pore structure [12, 13]. The regularity of subsequent nanostructures created using the AAO template as the host material is controlled by the ordering of the pore arrangement [14, 15]. One of the most significant features of the AAO templates is the tunability of cell size, and pore depth and diameter [16-19]. The diameter of pores (without widening process) depends on the used electrolyte and is related to the applied voltage of anodization and can be adapted in the range of about a few nanometers to several hundred nanometers (the corresponding cell size is in the range of about 25–800 nm) [20]. The AAO structure figuration is demonstrated in Figure 1, the anodization of high-purity Al foil creates a closely packed hexagonal cell array. These cells have a central cylindrical pore that is perpendicular to the surface, the pores are

distinguished from each other by the I_L consisting of Al_2O_3 [3].

In general, porous materials have more attraction attention recently for their significant optical properties and high surface area that allow to extend the light absorbance range and reduce the reflection which increases the efficiency of the light-dependent applications[21]. This study is a prof that the porous of aluminum oxide are improve the absorbance spectrum and opens up a new route to intense dependence of the applications related to solar energy conversion.

MATERIALS AND METHODS

Aluminum foil with high purity and thickness of around 220 µm was used to prepare AAO templates with high-ordered pores and various widths. By ethanol, acetone, ethanol, and DI water, respectively, Al foils were thoroughly cleaned initially. Al foil was anodized at a constant voltage of 40 V in 0.3 M oxalic acid at 10 °C for 6 h and 30 min for the first and second anodization, respectively. To achieve a specific P_D and I_L, the AAO templates surface was etched in a 5 wt% of H_3PO_4 solution at 30 °C, resulting AAO template with pore diameter around 50, 70, and 90 nm for 20, 30, and 40 min of the enlarging of pore diameter process, respectively. UV-vis-near IR spectroscopy measurements are carried out on a T70/T80 Series UV/vis spectrometer, to verify the experimentally observed transmittance and absorbance spectra of the fabricated AAO template. In order to better understand, numerical simulations were selected to simulate the distinguished design of AAO templates. Finite-Difference Time-Domain (FDTD) can explain such kind of light behavior in pore arrays materials [22-24], solving Maxwell's equations in time domain using FDTD provides another perspective to achieve simulations for both transmittance and absorbance spectra and investigating the enhancement of light interaction with the unique structure of the prepared AAO templates. The schematic diagram shown in Figure 1b illustrates the features of the FDTD and the AAO template

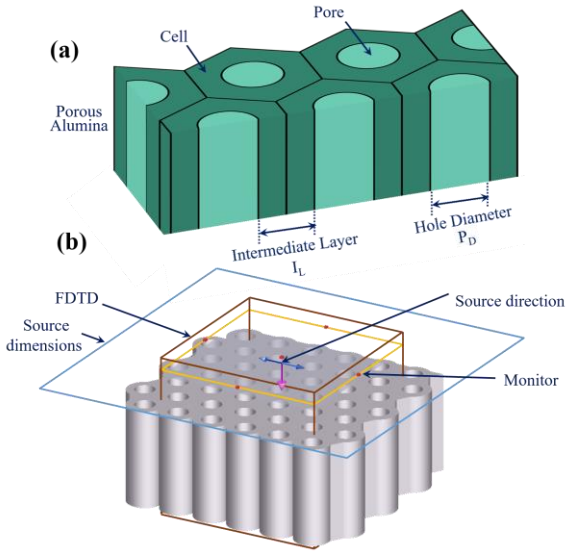

Figure 1. The schematic of the anodic aluminum oxide template.

RESULTS AND DISCUSSION

SEM images of the prepared AAO templates are presented in Figure 2. In a comparison with samples prepared after pore-widening for 20, 30, and 40 min, the pore diameter increases to 50, 70, and 90 nm, respectively, while the cell size keeps unchanged at 110 nm, and the average value of the pore diameter is steadily enlarged with increasing the time of the pore-widening process. Due to the etching effect of H_3PO_4 during the pore-widening process leading to thinning of the surface of the outer and inner (inside the pore) of AAO templates. This provides a suitable pathway to prepare an AAO template of precise pore diameter in the range below 100 nm of the cell size 110 nm that keep AAO templates stand in our experimental conditions [25, 26].

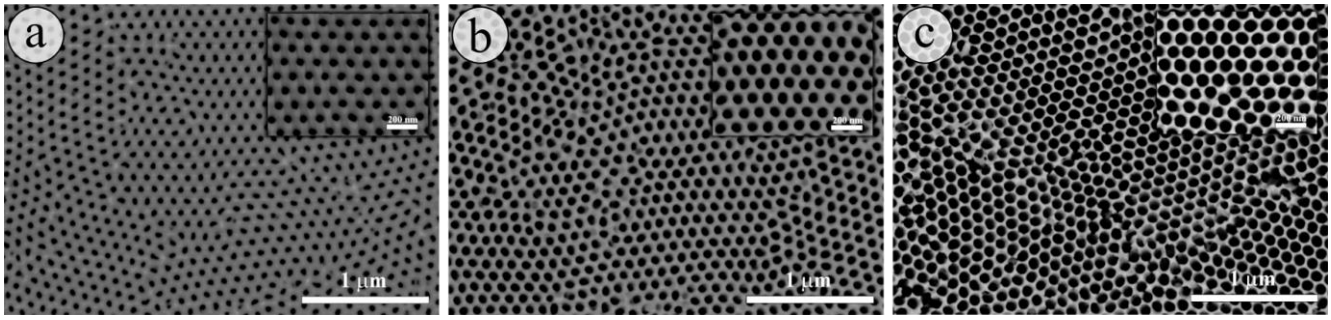

Figure 2. SEM images of the prepared AAO templates show the variation of pore diameters, the fabricated samples in images a, b, and c have different pore diameters of 50, 70, and 90 nm, respectively.

Table 1 determines the composition results of the EDX where the O atoms is 71.113 % and the Al atoms is 28.787 % which indicates that the film is alumina (Al_2O_3) with high purity and without any contaminations. Figure 3 displays the EDX line-scan profile from the red arrow in the SEM image, the Al and the O peaks ensure more evidence that the preparation of the AAO template was without any other contaminations.

Table 1. The presence of O and Al in the prepared AAO template was determined from EDX.

Element	*Atom Counts %*	*Atom Error %*
O- K	71.213	+/- 1.48
Al- K	28.787	+/- 0.29
Total	100	

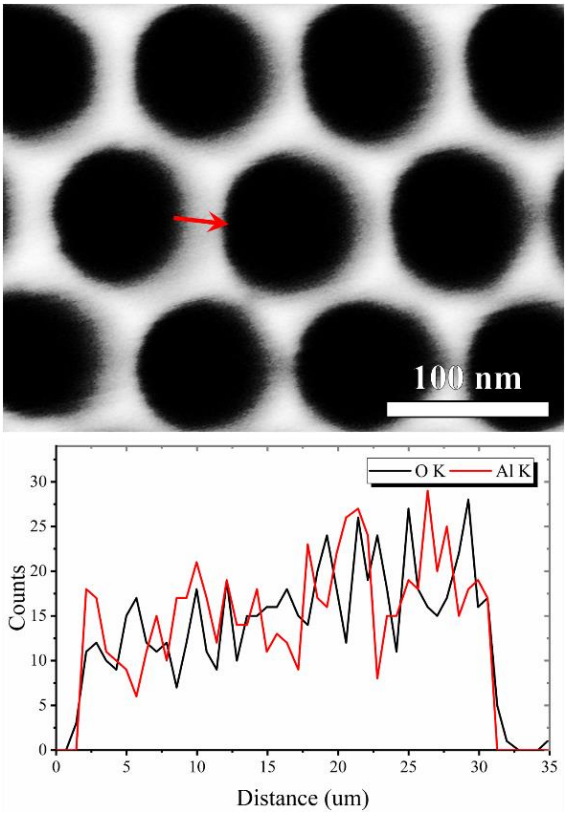

Figure 3. EDX spectrum of the presented SEM image showing the line scan profile of Al and O elements.

Figures 4a and 4b illustrate the transmittance and absorbance spectra, respectively. To measure the optical characteristics of the pore arrays of the AAO template, an UV-vis-near IR spectrometer (T70/T80 Series UV/Vis spectrometer) was adopted. The transmittance and absorbance spectra of AAO templates were virtually simulated using a three-dimensional FDTD solution. From documented experimentally refractive index data of the Al_2O_3 [27], the dielectric constants were provided and broad-band plane waves polarized linearly were incident perpendicularly onto individual hexagonal pore arrays of AAO template with periodic in-plane boundary conditions. AAO template pores with similar geometrical parameters to the prepared real AAO samples were used for all sets of the simulations. 5 nm of mesh size was used in the regions containing seven pores of the AAO template. To evaluate the transmittance, reflectance spectra, and then absorbance spectra of the AAO template and to generate field distribution maps at the desired wavelengths, field vectors were monitored in three-dimensional grid points. Both resulting transmittance and absorbance spectra of experimental and simulated show similar behavior in two regions (R_1 = 100-165 nm, R_2 = 170-800 nm), the slight deviations are probably just because of a few inevitable roughness of the real samples. At R_1 and for increasing the surface area by enlarging the diameter of the pores the light absorbance intensity increases also, despite the reduction of materials value (intermediate layer). Inversely, at R_2 and with reducing the pore diameter the light scattering rises due to a large surface area and movement spaces leading to a maximum reflection (probability of destructive interference increases) and reducing the transmittance driving to perform a higher absorbance of the lower diameter of AAO templates [28, 29].

Figure 5a shows the simulated electric field distribution around the nanopore structures at the top of the samples after being illuminated by the photons at 216 nm. The electric field intensity moves around the pores and inside the material of AAO templates, implying that the interaction between the photons and the nanoporous materials occurs on the surface of the intermediate layer between two pores, and the dimensions of such nanostructure could impact the interaction. It can note that the field intensity around the pores becomes higher as the diameter increases due to the sensitivity of the electric field to the different geometric parameters [22, 23].

For further analysis, the curve for the enhancements of near-field intensity $|E_x^2|$ at the AAO templates surface was plotted, Figure 5b. The $|E_x^2|$ dictates that the electric field decays when decreasing the pore diameter and improves when

increasing the intermediate layer, in other words at λ = 216 nm, P_D = 50 nm, and I_L= 60 nm, the absorbance becomes higher, and vice versa at P_D = 90 nm and I_L = 20 nm, the electric field optimized resulting lower photon absorption.

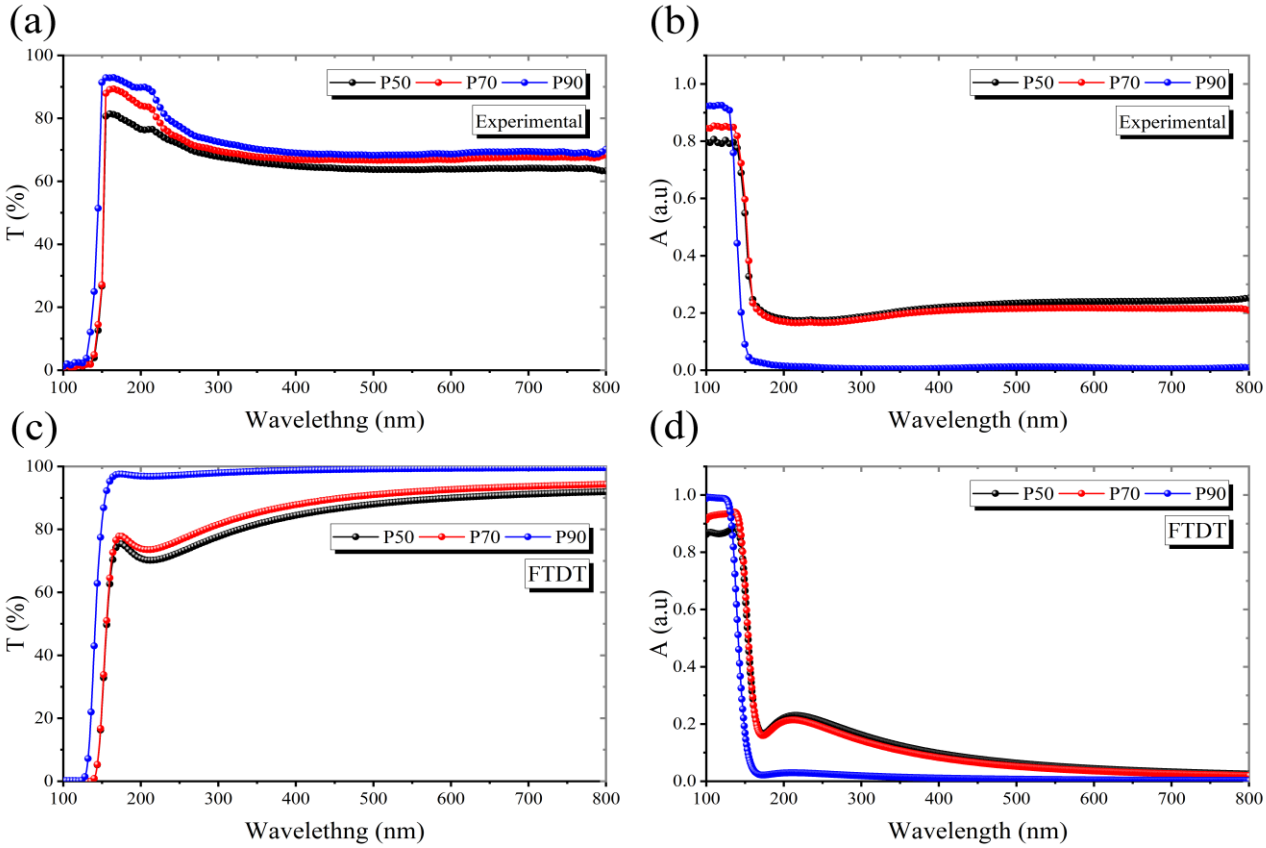

Figure 4. a and b Experimental transmittance and absorbance spectra of the prepared AAO templates, respectively, c and d Simulated transmittance and absorbance spectra of the designed structure of AAO templates, respectively.

When the samples are irradiated by photons at 216 nm, depicts the simulated electric field distribution around the nanopore structures and perspectives. Indicating that the interaction between photons and Al_2O_3 occurs on the surface of the intermediate layer between two pores and that the geometric properties of such a nanostructure may have an impact on the interaction, the electric field intensity moves around the pores and inside the material of AAO templates. It is simple to find that the field strength surrounding the pores gets higher as the diameter grows by comparing the electric fields of the samples with various geometrical characteristics [28].

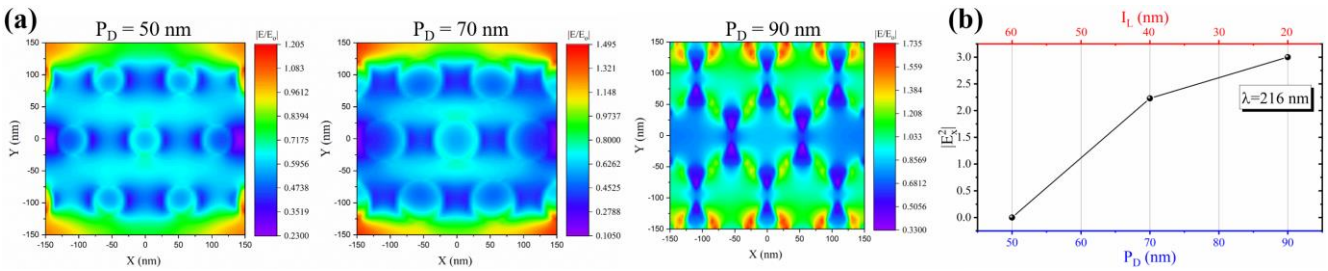

Figure 5. a) FDTD simulation of electric field intensity distribution illuminated by 216 nm showing x-y views of P_D = 50 nm, P_D = 70 nm, and P_D = 90 nm. b) FDTD calculated $|E_x^2|$ enhancement at x-y views and the inner surface of AAO template as a function of the intermediate layer (red top) and pore diameter (blue down) of Al_2O_3 under the same illumination.

CONCLUSIONS

Under a constant AAO template were successfully prepared using a two-step anodizing method. Optimal pore-widening conditions result in precise pore diameter and the intermediate layer. The absorbance spectrum of the AAO templates can be enhanced by combining a certain pore diameter with a particular intermediate layer, concluding that the ordered pore arrays could enhance many light-related applications such as solar energy applications (as an antireflective layer), water

oxidation (photocatalyst), or even LEDs, …etc. Further investigation to realize more evidence for the outcome of the experimental data, three-dimensional full-field FDTD techniques were used to replicate the optical characteristics of AAO templates, which resulted in a good match experimental result and offer a realistic light interaction with AAO template pore arrays understanding.

ACKNOWLEDGMENT

The authors would like to acknowledge RES laboratory, department of physics, college of sciences, Mustansiriyah University, Baghdad, Iraq.

Disclosure and conflict of interest: The authors declare that they have no conflicts of interest.

REFERENCES

[1] L. Hu, H. Wu, and Y. Cui, "Metal nanogrids, nanowires, and nanofibers for transparent electrodes," MRS Bulletin, vol. 36, no. 10, pp. 760-765, 2011. https://doi.org/10.1557/mrs.2011.234

[2] H. Zhao, L. Liu, Y. Fang, R. Vellacheri, and Y. Lei, "Nickel nanopore arrays as promising current collectors for constructing solid-state supercapacitors with ultrahigh rate performance," Frontiers of Chemical Science and Engineering, vol. 12, no. 3, pp. 339-345, 2018. https://doi.org/10.1007/s11705-018-1699-6

[3] A. Al-Haddad, Z. Zhan, C. Wang, S. Tarish, R. Vellacheria, and Y. Lei, "Facile Transferring of Wafer-Scale Ultrathin Alumina Membranes onto Substrates for Nanostructure Patterning," ACS Nano, vol. 9, no. 8, pp. 8584-8591, 2015. https://doi.org/10.1021/acsnano.5b03789

[4] L. Liang et al., "Large-scale highly ordered Sb nanorod array anodes with high capacity and rate capability for sodium-ion batteries," Energy & Environmental Science, vol. 8, no. 10, pp. 2954-2962, 2015. https://doi.org/10.1039/C5EE00878F

[5] A. Al-Haddad et al., "TiN@Al2O3/Al nanocapacitor based on anodic aluminum oxide template," in AIP Conference Proceedings, 2020, vol. 2307, no. 1, p. 020016: AIP Publishing LLC. https://doi.org/10.1063/5.0033137

[6] X. Wang et al., "Ordered single-crystalline Bi nanowire arrays embedded in nanochannels of anodic alumina membranes," Journal of Physics D: Applied Physics, vol. 34, no. 3, p. 418, 2001. https://doi.org/10.1088/0022-3727/34/3/328

[7] L. Li, "Influence of phosphorous acid on electrodeposition of cobalt in pores of porous anodic films of aluminum," Journal of materials science letters, vol. 20, no. 15, pp. 1459-1461, 2001. https://doi.org/10.1023/A:1011632703263

[8] T. Gao et al., "Template synthesis of single-crystal Cu nanowire arrays by electrodeposition," Applied Physics A, vol. 73, no. 2, pp. 251-254, 2001. https://doi.org/10.1007/s003390100910

[9] Y. Li, G. Meng, L. Zhang, and F. Phillipp, "Ordered semiconductor ZnO nanowire arrays and their photoluminescence properties," Applied Physics Letters, vol. 76, no. 15, pp. 2011-2013, 2000. https://doi.org/10.1063/1.126238

[10] D. Xu, X. Shi, G. Guo, L. Gui, and Y. Tang, "Electrochemical preparation of CdSe nanowire arrays," The Journal of Physical Chemistry B, vol. 104, no. 21, pp. 5061-5063, 2000. https://doi.org/10.1021/jp9930402

[11] J. Zhang, L. Zhang, X. Wang, C. Liang, X. Peng, and Y. Wang, "Fabrication and photoluminescence of ordered GaN nanowire arrays," The Journal of Chemical Physics, vol. 115, no. 13, pp. 5714-5717, 2001. https://doi.org/10.1063/1.1407005

[12] H. Masuda and K. Fukuda, "Ordered metal nanohole arrays made by a two-step replication of honeycomb structures of anodic alumina," Science, vol. 268, no. 5216, pp. 1466-1468, 1995. https://doi.org/10.1126/science.268.5216.1466

[13] H. K. Habool, R. S. Sabry, and A. H. Al-Fouadi, "Novel fabrication of Ag nanostructures by template-based and photo reduction method," Al-Mustansiriyah Journal of Science, vol. 29, no. 1, 2018. https://doi.org/10.23851/mjs.v29i1.304

[14] X. Wang and G.-R. Han, "Fabrication and characterization of anodic aluminum oxide template," Microelectronic Engineering, vol. 66, no. 1-4, pp. 166-170, 2003. https://doi.org/10.1016/S0167-9317(03)00042-X

[15] A. K. Albarazanchi, A. Al-Haddad, and M. F. Sultan, "Plasmonic Enhancement Mechanism of Template-Based Synthesized Au@TiO2 Nanodiscs," ChemNanoMat, vol. 7, no. 1, pp. 27-33, 2021. https://doi.org/10.1002/cnma.202000513

[16] O. Jessensky, F. Müller, and U. Gösele, "Self-organized formation of hexagonal pore arrays in anodic alumina," Applied Physics Letters, vol. 72, no. 10, pp. 1173-1175, 1998. https://doi.org/10.1063/1.121004

[17] D. Routkevitch, A. Tager, J. Haruyama, D. Almawlawi, M. Moskovits, and J. M. Xu, "Nonlithographic nano-wire arrays: fabrication, physics, and device applications," IEEE transactions on electron devices, vol. 43, no. 10, pp. 1646-1658, 1996. https://doi.org/10.1109/16.536810

[18] H. Masuda, H. Yamada, M. Satoh, H. Asoh, M. Nakao, and T. Tamamura, "Highly ordered nanochannel-array architecture in anodic alumina," Applied Physics Letters, vol. 71, no. 19, pp. 2770-2772, 1997. https://doi.org/10.1063/1.120128

[19] J. C. Hulteen and C. R. Martin, "A general template-based method for the preparation of nanomaterials," Journal of Materials Chemistry, vol. 7, no. 7, pp. 1075-1087, 1997. https://doi.org/10.1039/a700027h

[20] Y. Lei, W. Cai, and G. J. P. i. M. S. Wilde, "Highly ordered nanostructures with tunable size, shape and properties: A new way to surface nano-patterning using ultra-thin alumina masks," vol. 52, no. 4, pp. 465-539, 2007. https://doi.org/10.1016/j.pmatsci.2006.07.002

[21] F. M. Hussein, "Synthesis and Characterization of Nanostructure Tio2/Anthraquenone (AQ) Prepared by Sol-Gel Method," Al-Mustansiriyah Journal of Science, vol. 28, no. 1, pp. 76-83, 2017. https://doi.org/10.23851/mjs.v28i1.316

[22] A. Al-Haddad et al., "Dimensional Dependence of the Optical Absorption Band Edge of TiO2 Nanotube Arrays beyond the Quantum Effect," The Journal of Physical Chemistry C, vol. 119, no. 28, pp. 16331-16337, 2015. https://doi.org/10.1021/acs.jpcc.5b02665

[23] S. Tarish et al., "The shift of the optical absorption band edge of ZnO/ZnS core/shell nanotube arrays beyond quantum effects," Journal of Materials Chemistry C, vol. 4, no. 7, pp. 1369-1374, 2016. https://doi.org/10.1039/C5TC04152J

[24] S. Tarish et al., "Highly efficient biosensors by using well-ordered ZnO/ZnS core/shell nanotube arrays," Nanotechnology, vol. 28, no. 40, p. 405501, 2017. https://doi.org/10.1088/1361-6528/aa82b0

[25] C. R. Martin, "Membrane-based synthesis of nanomaterials," Chemistry of materials, vol. 8, no. 8, pp. 1739-1746, 1996. https://doi.org/10.1021/cm960166s

[26] F. Li, L. Zhang, and R. M. Metzger, "On the growth of highly ordered pores in anodized aluminum oxide," Chemistry of Materials, vol. 10, no. 9, pp. 2470-2480, 1998. https://doi.org/10.1021/cm980163a

[27] I. H. Malitson and M. J. Dodge, "Refractive-index and birefringence of synthetic sapphire," in Journal of the Optical Society of America, 1972, vol. 62, no. 11, pp. 1405-1405.

[28] A. V. Malinka, "Light scattering in porous materials: Geometrical optics and stereological approach," Journal of Quantitative Spectroscopy and Radiative Transfer, vol. 141, pp. 14-23, 2014. https://doi.org/10.1016/j.jqsrt.2014.02.022

[29] H. Yamashita et al., "Single-site and nano-confined photocatalysts designed in porous materials for environmental uses and solar fuels," Chemical Society Reviews, vol. 47, no. 22, pp. 8072-8096, 2018. https://doi.org/10.1039/C8CS00341F

How to Cite

R. M. Hameed, A. Al-Haddad, and A. K. H. Albarazanchi, “Pore Size Dependence of Optical Absorption Enhancement in Porous Anodic Aluminum Oxide”, *Al-Mustansiriyah Journal of Science*, vol. 33, no. 4, pp. 162–167, Dec. 2022.